 Cytometry 40:219–229 (2000)

Simultaneous Recording of Calcium Transients and Reactive Oxygen Intermediates of Human Polymorphonuclear Granulocytes in Response to Formyl-Met-Leu-Phe and the Environmental Agent Sulfite

Werner Grundler,[1]* Peter Dirscherl,[1] Ingrid Beck-Speier,[2] Wolfgang Beisker,[1] Andreas Stampfl,[3] Ingrid Zimmermann,[1] and Konrad Maier[2]

[1]Flow Cytometry Group, GSF - National Research Center for Environment and Health, Neuherberg, Germany
[2]Institute of Inhalation Biology, GSF - National Research Center for Environment and Health, Neuherberg, Germany
[3]Institute of Toxicology, GSF - National Research Center for Environment and Health, Neuherberg, Germany

Received 10 August 1999; Revision Received 1 February 2000; Accepted 22 March 2000

Background: Human polymorphonuclear granulocytes (PMN) are an essential component in the immunological defense network against a variety of harmful pathogens. We have studied the effects of the airborne pollutant sulfite on the calcium metabolism and respiratory burst of these cells simultaneously.

Methods: A flow cytometric method was developed using the fluochromes Indo-1 and DHR-123. This method allowed us to investigate the real-time kinetics of intracellular free calcium and reactive oxygen intermediates in viable cells with a temporal resolution of 1 s over a time course of 17 min. An additional feature was the possibility to discriminate between reacting and nonreacting cells after treatment with defined stimuli, thus gaining additional insight into the behavior of cell subpopulations.

Results: We analyzed the effects of sulfite on PMN before and after stimulation with formyl-Met-Leu-Phe (FMLP). Treatment with sulfite alone (0.001–1 mM) caused a small, nontransient increase in intracellular calcium. Preincubation with sulfite reduced the maximal calcium response elicited by FMLP. A significant increase in steady-state calcium levels after stimulation with FMLP was observed after treatment with sulfite in concentrations of 10 and 100 mM. Regarding the respiratory burst, treatment with sulfite alone in concentrations of 0.001–1 mM induced a significant increase in DHR-123–derived fluorescence, whereas concentrations of 5 and 10 mM caused a significant depression of this fluorescence below baseline values. Sulfite caused a maximal twofold increase of DHR-123–derived fluorescence compared with the FMLP response. Similar results were obtained after preincubation with sulfite before treatment with FMLP, showing that the effect of sulfite on the respiratory burst was additive to the FMLP response. Regarding the fractions of responding cells, treatment with sulfite up to 1 mM induced a concentration-dependent increase of burst-reactive PMN, whereas preincubation before stimulation with FMLP showed no correlation between sulfite concentration and fraction of burst-reacting cells.

Conclusions: By simultaneous registration of $[Ca^{2+}]_i$ and $[H_2O_2]_i$ of PMN after treatment with FMLP and sulfite, the essential responses were already observed within a short time interval (15 min). Striking differences were found in the response of calcium as second messenger and respiratory burst in PMN treated with sulfite. Until a critical concentration (0.5–1 mM), sulfite caused a concentration-dependent increase of $[H_2O_2]_i$, in addition to the FMLP-induced response. The $[Ca^{2+}]_i$ changes induced by sulfite alone, however, were found to be small and showed no correlation with the respiratory burst response. Cytometry 40:219–229, 2000. © 2000 Wiley-Liss, Inc.

Key terms: calcium; respiratory burst; flow cytometry; human polymorphonuclear granulocytes; sulfite; Indo-1; DHR-123

Human polymorphonuclear granulocytes (PMN) play a vital role in host defense against a variety of noxes. Normally localized in the peripheral blood and attached to blood vessels, these cells also have the ability to translocate via stimulus gradient-dependent migration into the

*Correspondence to: Dr. Werner Grundler, GSF—National Research Center for Environment and Health, Flow Cytometry Group, Ingolstädter Landstr. 1, 85764 Neuherberg, Germany.

lung. Here, they have the task of attacking and removing pathogens (1) in coordination with other cells such as alveolar macrophages controlled through a complex network of cytokines and lipid mediators.

To fulfill these requirements, a variety of cellular functions, such as migration, phagocytosis, bacterial killing, and respiratory burst, have to be performed under tight spatial and temporal coordination. Therefore, signal transduction has to allow differentiated reactions upon a variety of stimuli or, as termed by Hallet and Lloyds (2), these cells have to work in a multiple input-multiple output mode. Impairment of these cellular functions may result, on the one hand, in an inability to defend against pathogens, e.g., chronic granulomatous disease (CGD), where a genetic defect results in the inability to perform respiratory burst and therefore in bacterial killing (3). On the other hand, a prolonged activation, caused by retarded apoptosis or induced by environmental agents, may have detrimental effects on surrounding cellular and extracellular tissues. It has been shown that sulfite as a component of airborne pollution modulates the respiratory burst of PMN (4–7). Beck-Speier et al. (4) found a stimulation in the production of reactive oxygen metabolites with sulfite in concentrations up to 1 mM, but not with 10 mM sulfite. Depletion of oxidative burst by sulfite at a concentration of 10 mM is possibly based on a prominent loss of adenosine triphosphate (ATP; 8). In contrast, Labbe et al. (6) recently reported a substantially higher stimulation of the burst response after 10 mM compared to 1 mM sulfite. This contradictory result may originate in the different methodological approaches applied to respiratory burst analysis.

To further investigate the effects of sulfite as a component of airborne pollution on viable PMN, we developed a multiparameter flow cytometric assay to simultaneously investigate the kinetics of Ca^{2+} homeostasis and respiratory burst using the fluorochromes Indo-1 (9) and DHR-123 (10). The second messenger Ca^{2+} plays a major role in various cell functions like migration, phagocytosis, apoptosis, and respiratory burst. Ca^{2+} might be disturbed by exogenous noxes like airborne pollutants, thus causing pathophysiological irritations.

In this methodological study, we present an assay that supports investigations regarding the influence of the second messenger Ca^{2+} on the respiratory burst during treatment with a prominent air pollutant. With this assay, we were able to demonstrate that stimulation of the respiratory burst of PMN by sulfite is not preceeded by a significant Ca^{2+} transient.

MATERIALS AND METHODS

Blood Sampling

Venous blood samples were taken with a syringe prefilled with 6 mg sodium-heparinate (Vacutainer, Becton-Dickinson, Heidelberg, Germany) per milliliter of blood. Peripheral blood leukocytes (PBL) were separated from erythrocytes and debris by discontinuous density centrifugation (30 min, 400 × g, room temperature [RT]) using Polymorphprep (Gibco, Eggenstein, Germany). PBL harvested from the interface were suspended in RPMI without Ca^{2+} (Gibco), washed (10 min, 175 × g, RT), and purified from remaining erythrocytes by hypotonic lysis with aqua dest. After an additional washing step, an aliquot of the cell suspension was stained with 0.5% trypan blue solution (Serva, Heidelberg, Germany) to determine viability. Overall leukocyte numbers were quantified by use of a hemocytometer chamber. For storage, cells were suspended in PBS with Ca^{2+} and Mg^{2+} (1 mM $CaCl_2$; 0.5 mM $MgCl_2$ $6H_2O$) and 0.1% glucose.

Cell Staining

For Ca^{2+} measurements, cells were loaded with 5 μM Indo-1 AM (Sigma, no. I-3261, Deisenhofen, Germany) per 1×10^6 cells in RPMI without phenolred for 25 min at 37°C and 5% CO_2 . Cells were washed twice by centrifugation for 5 min at 175 × g and finally diluted to a concentration of 0.33×10^6 cells per milliliter. To discriminate between viable and dead cells, the cell suspension was stained with 3 μg/ml propidium iodide (PI; Sigma, no. P-4170).

Until further treatment and flow cytometric measurement, the cell suspension was filtered by a 37-μm meshed sterile gauze and stored in cytometer tubes (Falcon no. 2052, Becton-Dickinson) with 0.33×10^6 cells in 1 ml RPMI without phenolred up to 6 h at RT in the dark.

For determination of reactive oxygen intermediates (ROI), cells (0.33×10^6 cells/ml) were preincubated for 1 min at 37°C just before use. Thereafter, they were stained with 15 μM dihydrorhodamine 123 (DHR-123; Mobitec, Göttingen, Germany) for 9 min at the same temperature. Cells were slightly shaken to minimize the known time-dependent increase of minute quantities of the DHR-123–derived fluorescence even in untreated cells. Upon oxidation, DHR-123 is finally transformed to the fluorescent compound rhodamine-123 (R-123). This cationic dye is retained in the cell by negative charges at least for 2 h as experimentally tested.

Treatment and Stimulation of Cells

Stimulation of cell suspensions was performed with final concentrations of 10^{-7} M formyl-Met-Leu-Phe (FMLP), 160 nM phorbol myristate acetate (PMA), and 3 μM ionophore A23187 (all Sigma); sulfite was used in concentrations of 0.001–100 mM. To take into account possible variations of cellular functions or staining effects, sham-stimulated (with phosphate-buffered saline [PBS]) cells were analyzed in regular intervals and defined as control cells.

Thermostatted Sample Tube Holder

Temperature regulation and stabilization are essential requirements for analyzing the kinetic properties in living cells by flow cytometry. Small temperature variations (maximum ± 0.1°C) for the sample tube solution should be achieved over long time periods (days) despite variation in RT. The thermostatted sample tube holder developed by us is described and shown elsewhere (11). Briefly, a 5-min warming up time reduces the temperature difference between the initial temperature (RT) of the

sample tube solution and the final 37°C of the sample tube solution to a value smaller than 1%.

Mode of Adding the Stimulants

Interruption-free data recording during volume-controlled injection of stimulating or modifying chemicals, eventually for several times per run, is necessary to optimize time-dependent registration of kinetic cellular parameters using flow cytometry. These requirements are fulfilled by use of Hamilton microliter syringes (10, 25, and 100 μl; Hamilton GmbH, Darmstadt, Germany), equipped with specially sized (length 120 mm, inner diameter 150 μm) stainless steel needles, with a liquid discharge accuracy better than 0.1%. To enable an adequate, nearly vertical insertion direction of the needle, the original Becton-Dickinson fabricated sample tube head was replaced by a modified one described elsewhere (11). This setup enables an interruption-free data registration in intervals, as used here, of 1 s. The delay time between stimulation and registration remains smaller than 3 s, due to the short transport time necessary from tube to nozzle by applying a reproducible (pressure difference 1 atm) boost procedure. Additionally, a standardized gentle stirring procedure was performed to avoid mechanically induced alterations of cellular calcium homeostasis.

Flow Cytometry

Fluorescence measurements. A FACSTARPLUS flow cytometer (Becton-Dickinson, Sunnyvale, CA [BD]) was used for simultaneous measurements of two cellular scatter parameters and four fluorescence signals over a time period of 1,024 s for one sample with a data acquisition interval of 1 s.

An argon ion laser (488 nm line, 1,000 mW, Innova 90, Coherent, Dieburg, Germany) was used for the generation of the two scatter signals as well as for the excitation of PI and R-123 fluorescence. The pulse heights of both forward light scatter (FSC) and 90-degree side scatter (SSC) were collected using 488-nm band pass filters (BD, 488 BP 10). PI and R-123 emissions were recorded with a combination of KV 550 and OG 590 filters and a 530-nm band pass filter (BD, 530 BP 30, Schott, Mainz, Germany). Signal separation was performed by a dichroic mirror (BD, DM 560) as beam splitter.

The second laser (argon ion laser, Innova 100, Coherent), adjusted to the ultraviolet (UV) multilines 351.1–363.8 nm (500 mW), was used for the excitation of the ratiometric Ca^{2+} indicator, Indo-1. Violet and green fluorescence signals of the Indo-1 fluorochrome were separated by a long pass beam splitter (BD, LP430 DC) and recorded by two band pass filters of 395/25 nm (BD, 395BP25) and 530/30 nm (BD, 530BP30). This recording wavelength was selected for optimizing the sensitivity of the Ca^{2+}-dependent Indo-1 ratio shifts.

Data recording. Data recording was done with a HP 9000 Series 300 Computer (Hewlett-Packard, Corvallis, OR) in list mode using the FACSTARPLUS research software (BD, Lysys II). Electronic pulses were triggered on the FSC signal set to a threshold level excluding debris-related signals with a flow rate of 150–200 cells per second. Bivariate FSC-PI pulse high signals were registered on a logarithmic scale.

On a double linear plot, the pulse area signals of the violet and green Indo-1 fluorescence were recorded to observe the relative pulse amplitude of the single signals, which are masked when their ratio alone is registered as a signal proportional to the Ca^{2+} concentration. The ratio of both Indo-1 signals was calculated in real time and plotted against time on a linear scale with a total registration time of 1,024 s. Simultaneously, the time-dependent DHR-123–derived fluorescence was recorded and displayed on a linear/logarithmic plot.

Data of the eight parameter list mode files (2–3 MB each) were transferred to an MS-DOS IBM-compatible computer system by FASTNET software (BD).

Data Analysis

Subsequent data handling and color graphic display of results were performed with the Data Analysis Software DAS V4.19 (12). For every list mode file, a standard data analysis procedure was performed by means of three specified batch programs, composed of elements of the DAS package.

First, the measured ratio of the real-time data of both Indo-1 signals in the list mode file was replaced by the calculated numerical quotient of both Indo-1 fluorescence intensity values. Then, by interactive gating procedures, the necessary gates were established.

By a third standard routine, the mean, SD, and percentage of reactive cells of the fluorescence signals related to intracellular calcium and to the fluorescence signal excited by laser one (PI or R-123 fluorescence) were calculated for every time channel. For selected time intervals, statistical analysis for significance after Behrens-Fischer (13) was performed to compare differences of distributions with uneven variances. Values of $P < 0.05$ were considered significant and values of $P < 0.01$ were highly significant.

RESULTS

Dot-Plot Data Recording and Gating

Real-time data recording of PBL was performed by using a bivariate plot (FSC log versus PI fluorescence log) for gating out debris and discrimination between viable and dead cells. As shown in Figure 1a, cells with a relative PI fluorescence greater than 1,000 were defined as dead cells. Leukocyte subpopulations were defined in an SSC versus Indo-1 fluorescence 395-nm plot (Fig. 1b) showing lymphocytes (gate 1, G1), monocytes (G2), and neutrophils (G3). Nonviable cells are here recognized by having virtually no Indo-1 395 nm fluorescence. "All cells" are defined as G1+G2+G3.

Indo-1 fluorescence. Alterations of Ca^{2+}-related Indo-1 signals in PMN (G3) after stimulation with FMLP are plotted in Figure 2. After stimulation with 10^{-7} M FMLP, the Indo-1 395 nm fluorescence increased (Fig. 2a), whereas the corresponding Indo-1 530 nm fluorescence decreased simultaneously (Fig. 2b). The ratio of these two

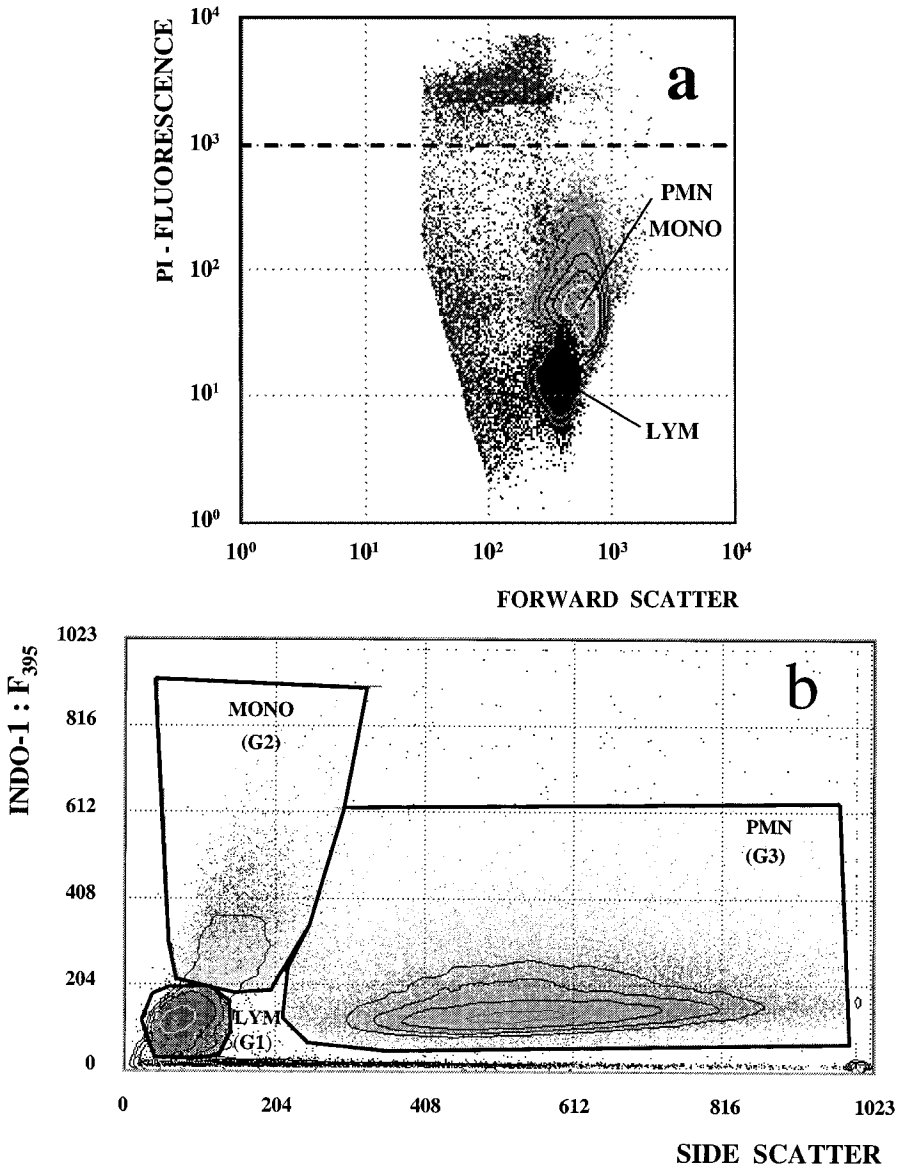

FIG. 1. **a:** Gating out debris and discrimination between viable (PI-negative) and dead (PI-positive) cells. Cells with a PI fluorescence greater than 1,000 (dashed line) are defined as dead cells. **b:** Definition of leukocyte subpopulations on the basis of granularity and Indo-1 395 nm fluorescence: lymphocytes (G1), monocytes (G2), and neutrophils (G3).

signals (Indo-1 fluorescence 395 nm divided by Indo-1 fluorescence 530 nm) is proportional to the intracellular Ca^{2+} concentration $[Ca^{2+}]_i$. The absolute concentration values were calculated according to Grynkiewicz et al. (9) using a K_d of 250 nM after modification of some other constants (14) by calibration using flow cytometry and spectrofluorometry (for details, see ref. 9). The result of this Indo-1 fluorescence calibration procedure is that the relative ordinate values (e.g., in Figs. 3a or 4a) correspond numerically with the absolute $[Ca^{2+}]_i$ in nM with an uncertainty of about ±15%. If the ratio is plotted in a bivariate plot (Indo-1 fluorescence 395 nm versus Indo-1 fluorescence 530 nm), the changes and the extent of the inclination represent the dynamic extent of Ca^{2+}-related reactions (15).

As a further step in the analysis of Ca^{2+}-related events, time is plotted against the Indo-1 ratio (Fig. 3a). This plot includes all viable cells (PI-negative, G1+G2+G3). Ca^{2+}-nonresponding cells are defined by gate 4 for the range from 0 to 1,023 s (G4) with a defined threshold value, established by the mean Indo-1 ratio plus twofold SD before stimulation with 10^{-7} M FMLP. Control cells are defined by gate 6 (G6), representing all cells before stimulation. Gate 5 (G5) shows Ca^{2+}-responding cells before and after stimulation, which are, per definition, all cells minus G4.

DHR-123–derived fluorescence. In a comparable presentation, the simultaneously registered response of viable PBL due to the respiratory burst is shown in Figure 3b. It contains respiratory burst-nonresponding cells defined by gate 7 (G7) below a threshold value (mean of R123 fluorescence plus twofold SD). The threshold value is set up in the time course before stimulation with 10^{-7} M FMLP. Gate 8 (G8) contains all respiratory burst-responding cells before and after stimulation.

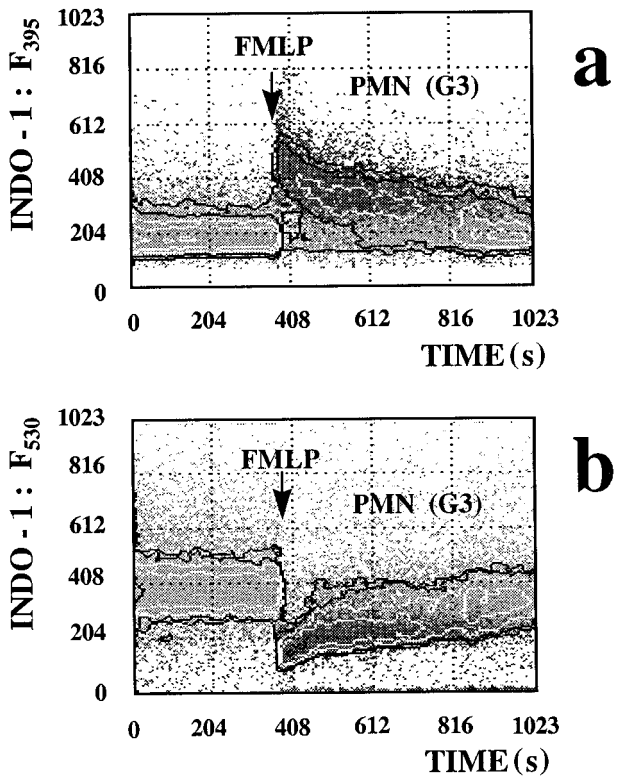

FIG. 2. Indo-1 signals of neutrophils (G3) after stimulation with 10^{-7} M FMLP over a time course of 17 min. **a:** Indo-1 395 nm fluorescence intensity. **b:** Indo-1 530 nm fluorescence intensity.

Kinetic Analysis of Indo-1 and DHR-123–Derived Fluorescence

Figure 4a shows the mean of the Indo-1 ratio signals per time channel calculated from 150 to 200 cells defined as the relative $[Ca^{2+}]_i$ for cells in G1, G2, and G3 over a time period of 17 min with a resolution of 1 s. Stimulation with 10^{-7} M FMLP is performed after 6 min. PMN and monocytes show a slightly different $[Ca^{2+}]_i$ kinetics after stimulation, whereas lymphocytes and PBS-treated PMN do not respond. As additional possibilities for quantification of the cellular response to the stimulus, the following parameters could be used: (1) relative maximum of $[Ca^{2+}]_i$ and (2) $[Ca^{2+}]_i$ between 900 and 1,023 s.

Dynamic changes of the mean R-123 fluorescence over 17 min are shown in Figure 4b, indicating respiratory burst-related H_2O_2 production in PMN and monocytes after stimulation with 10^{-7} M FMLP. Virtually no reaction is seen in lymphocytes and sham-stimulated PMN using PBS.

Analysis of Fractions of Responding Cells

The analysis of fractions of responding cells is an important feature for quantifying cellular responses. The percentage of responding cells in a subpopulation is defined as the number of reacting cells divided by the sum of reacting and nonreacting cells in this subpopulation. With regard to $[Ca^{2+}]_i$ (Fig. 5a), over 85% of PMN and nearly 40% of monocytes react upon stimulation with FMLP, albeit with different time dependence. No lymphocytes, as expected, respond to FMLP. (A total count analysis of this specific PBL population in Figure 5 showed that 58% were PMN, 17% monocytes, and 25% lymphocytes.)

Analysis of respiratory burst (Fig. 5b) indicates that more than 85% of PMN and nearly 50% of monocytes produce H_2O_2, whereas lymphocytes do not respond. Within the accuracy of the experiments, these data are in agreement with those of the Ca^{2+}-responding cell fractions.

Specificity of Indo-1 and DHR-123 Reactions

To investigate the specificity of reactions in double-loaded PMN, cells were stimulated with the ionophore A23187, eliciting maximal Ca^{2+} response or PMA as a trigger for receptor-independent maximal respiratory burst response. As plotted in Figure 6a with the mean and the 95% interval of the mean (paired *t*-test), maximum $[Ca^{2+}]_i$ response occurred almost immediately after stimulation with 3 μM ionophore A23187, whereas no respiratory burst reaction was observed simultaneously (Fig. 6b). In contrast, upon stimulation with 160 nM PMA, no $[Ca^{2+}]_i$ response was seen (Fig. 6c); respiratory burst, however, showed a gradual increase after a lag time (Fig. 6d). In both cases, PBS-stimulated PMN showed no reaction.

Effect of Sulfite on $[Ca^{2+}]_i$ and Respiratory Burst

Treatment of PMN with sulfite alone caused a spontaneous small, nonsignificant increase of $[Ca^{2+}]_i$. Figure 7a demonstrates this PMN response after stimulation with 0.1, 1.0, and 10 mM sulfite. For further analysis, data from cells measured in the time interval between 900 and 1,023 s were used and defined as the steady-state level of $[Ca^{2+}]_i$ (sst-Ca^{2+}) after stimulation. Addition of sulfite in different concentrations 5 min before stimulation with 10^{-7} M FMLP caused a reduction of the maximal $[Ca^{2+}]_i$ response and a small but nonsignificant increase in sst-Ca^{2+} (Fig. 7b). These results and additional data of maximal $[Ca^{2+}]_i$ response and sst-Ca^{2+} were used for the concentration-dependent analysis of sulfite on PMN. The sulfite-related increase of all sst-Ca^{2+} are summarized in Figure 7c.

The inserted error bars for the Ca^{2+} experiments (Figs. 7c,d) as well as for the burst-related relative H_2O_2 concentrations (Figs. 8b,d) are based on the experimentally defined confidence intervals (95% CI for the signal means per time channel) of the relevant runs as shown in Figure 6. After averaging these CI values over time (900–1,023 s or maximal response time intervals), error propagation and application of the Behrens-Fischer significance test (for distributions of unequal variances [13]) lead to the error bars inserted in the diagrams mentioned above.

Regarding the sst-Ca^{2+} of PMN, sulfite alone and treatment with sulfite (0.001–1 mM) 5 min before stimulation with FMLP enhanced the $[Ca^{2+}]_i$ only slightly. Sulfite alone in a concentration of 10 mM hardly had any effect on sst-Ca^{2+}, in contrast to the significant increase when given 5 min before FMLP. A drastic rise of sst-Ca^{2+} in

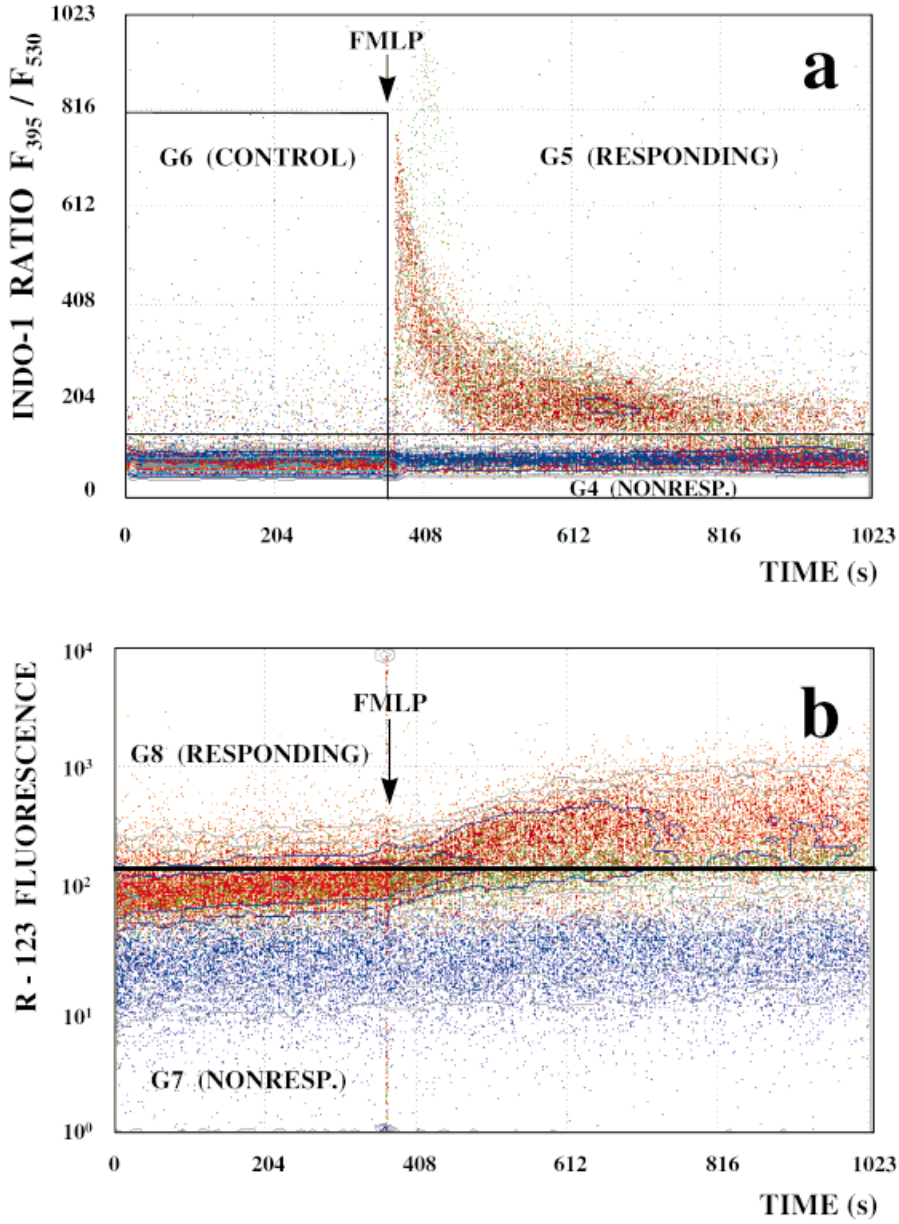

FIG. 3. Rationale of applied standardized interactive gating procedures of simultaneously recorded Indo-1 and R-123 fluorescence after stimulation of PBL with 10^{-7} M FMLP. **a:** Indo-1 ratio (Indo-1 395 nm divided by the Indo-1 530 nm fluorescence intensity) of all viable cells. Ca^{2+}-nonresponding cells are defined by gate 4 ranging from 0 to 1,023 s (G4), within a threshold value established by the mean Indo-1 ratio of control cells plus twofold SD. Control cells are defined by G6, representing all cells before stimulation. G5 (ranging from 0 to 1,023 s) shows Ca^{2+}-responding cells before and after stimulation. **b:** Due to R-123 fluorescence, respiratory burst-nonresponding cells are defined by G7 below a threshold value established by a similiar procedure as mentioned above. The threshold is set up in the time course before stimulation. G8 shows all respiratory burst-responding cells before and after stimulation.

viable PMN was caused by a sulfite concentration of 100 mM (Fig. 7c). As shown in Figure 7d, sulfite up to a concentration of 1 mM caused a slight reduction of the maximal Ca^{2+} response (related to the maximal $[Ca^{2+}]_i$ increase of control cells after FMLP stimulation [100%]). Sulfite in concentrations of 10 and 100 mM caused a significant reduction of the maximal Ca^{2+} response.

The influence of sulfite, given alone or during preincubation 5 min before FMLP stimulation, on the production of ROI during the respiratory burst of PMN is summarized in Figure 8. The time-dependent increase of the R-123 fluorescence caused by selected sulfite concentrations of 0.1, 1.0, and 10 mM is demonstrated in Figure 8a. The slightly increasing background signal (PBS injection) should be mentioned. As for the Ca^{2+} experiments before, the mean values of the burst signals out of the 900–1,023 s time interval are defined as steady-state values of $[H_2O_2]_i$ (sst-H_2O_2). Runs over a longer time scale have shown that at least 80% of the saturation value is achieved at this time point.

Figure 8b shows that treatment with sulfite, depending on its concentration, increased the sst-H_20_2, normalized by the baseline- corrected sst-H_2O_2 after FMLP stimulation alone. Maximal respiratory burst response was achieved by sulfite concentrations between 0.1 and 1 mM, whereas 10 mM sulfite led to a significant suppression of R-123 fluorescence below baseline values (Fig. 8a).

Corresponding to Figure 7b, the preincubation effects of selected sulfite concentrations on the burst response of PMN after FMLP stimulation are demonstrated in Figure 8c. Sst-H_2O_2 drawn versus sulfite concentrations are

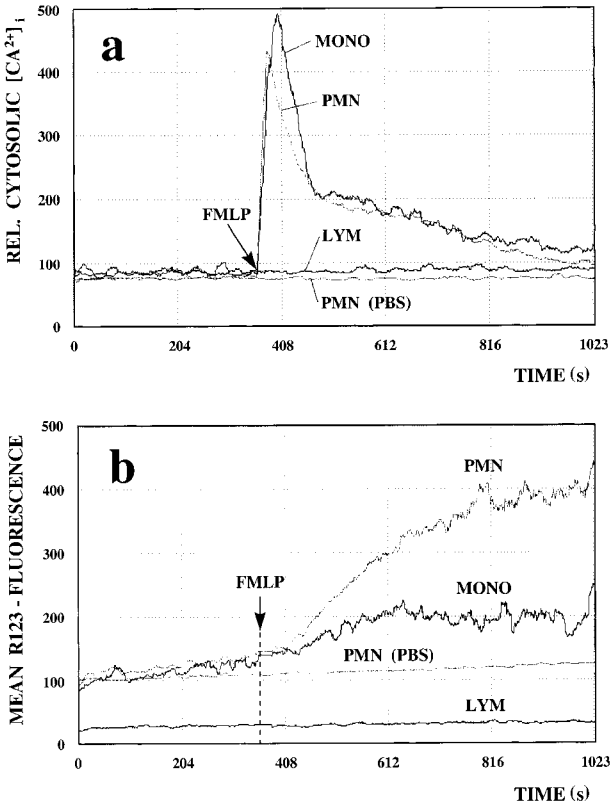

FIG. 4. Quantification of dot-plot data achieved by gating procedures during a time course of 17 min with a temporal resolution of 1 s (mean without SD for better presentation). **a:** After stimulation with FMLP (10^{-7} M), the relative cytosolic concentration of free $[Ca^{2+}]_i$ rises almost immediately in monocytes and neutrophils, whereas no reaction is seen in lymphocytes and PBS-stimulated neutrophils. Data from timepoints of maximal Ca^{2+} reaction and 900–1,023 s were taken for additional analysis. **b:** Dynamic changes of simultaneously recorded R-123 fluorescence from monocytes and neutrophils, as a marker for respiratory burst. Virtual no reaction is seen in lymphocytes and PBS-stimulated neutrophils. Mean data values from time intervals 900 to 1,023 s were taken for additional analysis.

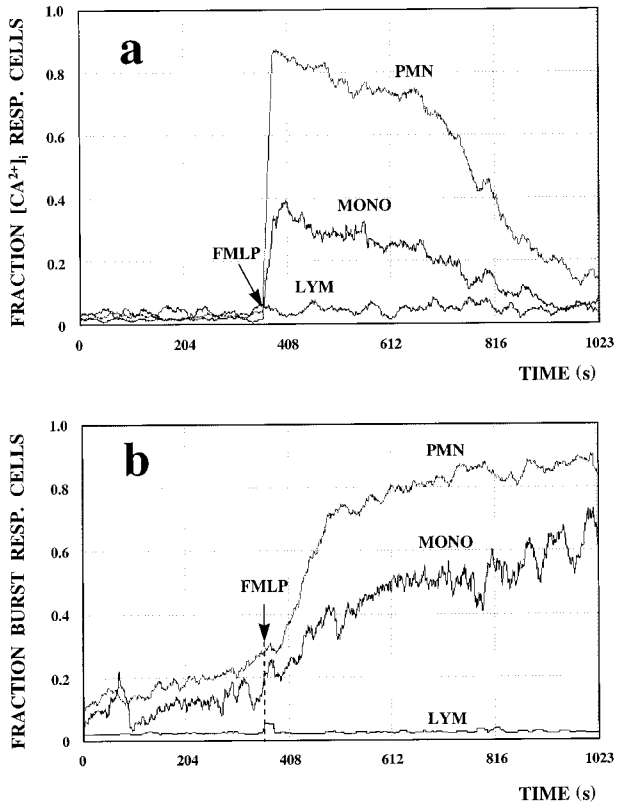

FIG. 5. Fraction of responding cells, defined as the ratio of reacting cells and all viable cells (see Figs. 3a and 3b for Ca^{2+} and burst response, respectively) after stimulation with 10^{-7} M FMLP during a time course of 17 min with a temporal resolution of 1 s. **a:** More than 85% of neutrophils (G3) and nearly 40% of monocytes (G2) are Ca^{2+} responsive, lymphocytes (G1) show no reaction. **b:** With respect to the respiratory burst, 85% neutrophils and about 50% monocytes are responding, no reaction is seen from lymphocytes.

shown in Figure 8d. As before, normalization of the sulfite-dependent increase of ROI production was performed by means of the FMLP-induced $[H_2O_2]_i$ increase (100%) in the corresponding control cell population.

Sulfite concentrations between 0.1 and 1.0 mM given 5 min before stimulation with 10^{-7} M FMLP enhanced the generation of ROI, whereas a sulfite concentration of 10 mM suppressed the FMLP-induced R-123 fluorescence. The sulfite-related enhancement of the ROI production was found to be additive to the FMLP effect (compare Figs. 8b,d).

Effects of Sulfite on the Amount of Responding Cells

Analysis of the fractions of reacting and nonreacting cells may offer an additional important feature for the evaluation of possible correlations between Ca^{2+} signals and ROI production, simultaneously measured in PMN after induction by different stimuli. The influence of sulfite on the fraction of burst-responding cells only is documented in Figure 9a. To define this fraction, the steady-state values of the reaction rates of the different runs are used (Figs. 5a,b), corrected by the R-123 baseline control level of the steady-state time interval. The biological variance of the blood donors, defined as the difference of the FMLP- responding fractions of every PMN preparation to the corresponding mean value of all runs (without sulfite), is corrected (see Fig. 9a legend). Sulfite alone up to 1 mM leads to a concentration-dependent increase of burst-reactive PMN, resulting in a maximum of 70% reacting cells, in contrast to only 10% burst-reactive PMN if treated with 10 mM sulfite. In contrast, no dose dependence was found between the sulfite concentration and the fraction of burst-reacting cells, when PMN are stimulated with FMLP after treatment with sulfite.

Finally, in Figure 9b, the fraction of Ca^{2+}-responding cells is compared with the fraction of burst responders by dividing the fraction of Ca^{2+} responders by the fraction of burst-reactive cells (Fig. 9a). In the control population, the 60% burst responders (Fig. 9a) are a fraction of the 90% Ca^{2+} responders (90%:60% = 1.5; Fig. 9b).

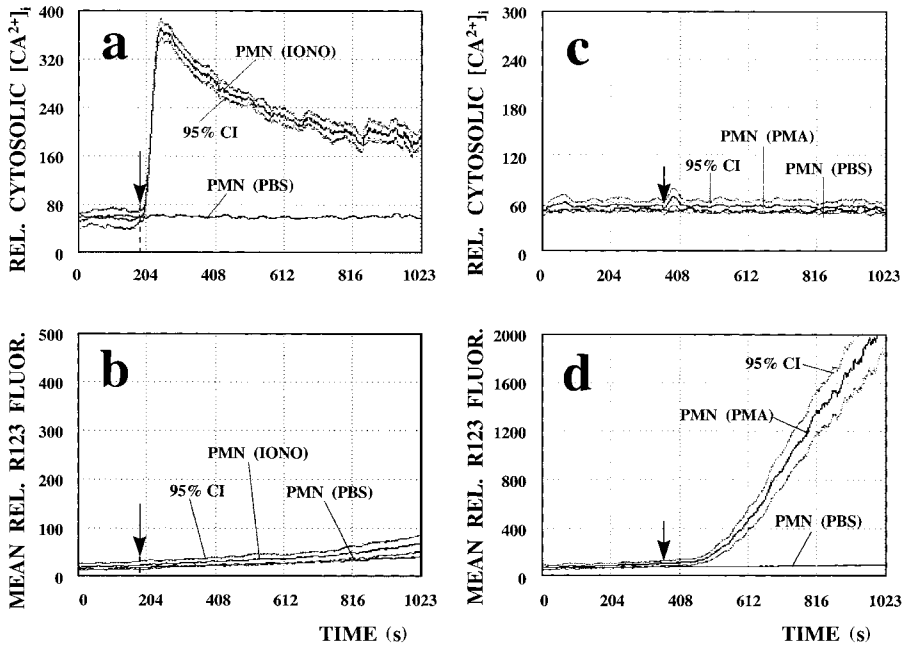

FIG. 6. Specificity of simultaneously recorded Indo-1 and R-123 reactions in neutrophils shown with mean time channel values and 95% confidence interval of the mean (paired student's t-test). Stimulation with 3 μM Ionophore (A23187): **a:** Maximum Ca^{2+} response; **b:** no respiratory burst is elicited. Stimulation with 160 nM PMA: **c:** no Ca^{2+} reaction; **d:** $[H_2O_2]_i$ shows a gradual rise.

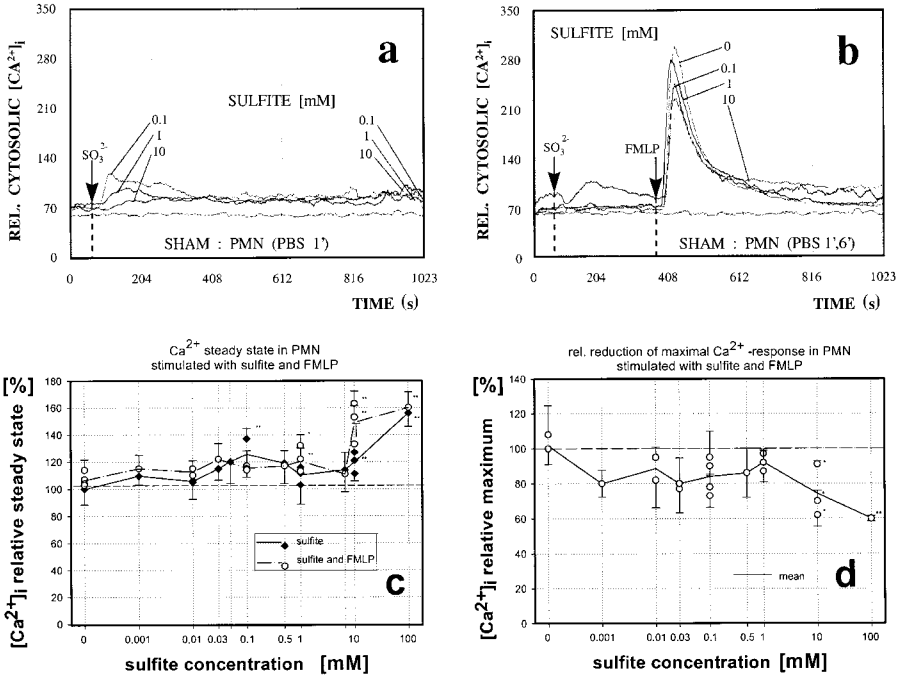

FIG. 7. Effects of sulfite on $[Ca^{2+}]_i$ in neutrophils. **a:** Stimulation with different concentrations of sulfite alone causes a small spontaneous rise of $[Ca^{2+}]_i$. The response in the time interval 900–1,023 s is defined as sst-Ca^{2+}. **b:** Preincubation with different concentrations of sulfite 5 min before additional stimulation with FMLP 10^{-7} M. Data from maximal Ca^{2+} response and sst-Ca^{2+} were used for additional analysis. **c:** Significant increase in relative sst-Ca^{2+} of neutrophils by sulfide in concentrations higher than 5 mM. The sst-Ca^{2+} of resting cells is set to 100%. **d:** In neutrophils, sulfite leads in concentrations of 10 and 100 mM to a significant reduction of maximal Ca^{2+} response defined as ratio of the baseline corrected peak Ca^{2+} levels induced by sulfide plus FMLP and by FMLP alone. $^*P < 0.05$; $^{**}P < 0.01$; the Behrens-Fischer significance test and error propagation define the error bars shown.

For the steady-state values (Fig. 9b, 17 min), no correlation between Ca^{2+}-reactive and burst-reactive cells was found if PMN were treated with sulfite up to 1 mM before stimulation with FMLP or treated with sulfite alone. With preincubation with 10 mM sulfite, almost the whole 30% burst-reacting fraction (Fig. 9a) had an elevated Ca^{2+} level.

Regarding the time point of maximal Ca^{2+} response, preincubation with sulfite up to 1 mM concentration led to a ratio of about 1 between percentages of Ca^{2+} and burst-responding cells. In other words, all burst-reactive cells are also Ca^{2+} reactive, caused obviously by the FMLP stimulation alone. At a sulfite concentration of 10 mM, 2.6-fold more cells showed Ca^{2+} reaction than respiratory burst, although this high sulfite concentration reduced the burst-reactive fraction to 30% only (Fig. 9a).

DISCUSSION

Measurements of alterations of the internal free Ca^{2+} concentration in neutrophils have been widely performed using a variety of fluorescent dyes, such as Fura-2 (16–21),

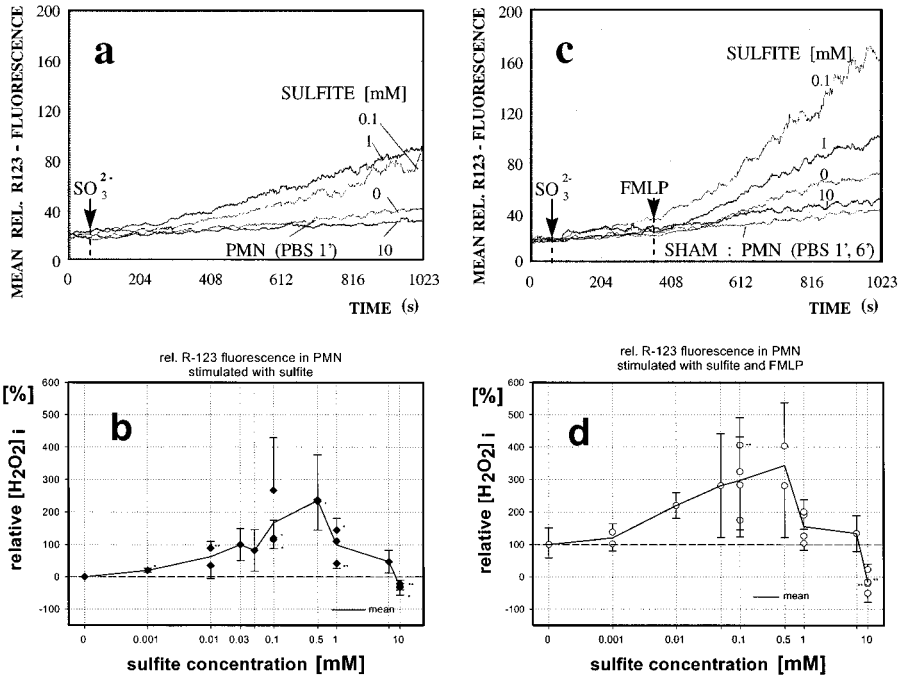

FIG. 8. Effects of sulfite on respiratory burst in neutrophils. **a:** Time-dependent relative mean R123 fluorescence in PMN, stimulated with different selected concentrations of sulfite. $[H_2O_2]_i$ levels from the time interval 900–1,023 s (sst-H_2O_2) were taken for additional analysis. **b:** Relative sst-H_2O_2 changes in neutrophils, related to FMLP-induced sst-H_2O_2 (set to 100%). Sulfite alone in concentrations from 0.001 to 1.0 mM induces significantly respiratory burst in neutrophils. Concentrations of 10 mM lead to a significant depression of respiratory burst activity below baseline values. **c:** Priming by different concentrations of sulfite 5 min before stimulation with FMLP 10^{-7} M. Data from time interval 900 to 1,023 s were taken for additional analysis (sst-H_2O_2). **d:** Preincubation with sulfite in concentrations of 0.001–0.5 mM causes an increase of FMLP-induced respiratory burst. The sulfite-related increase is additive to the FMLP effect (see b). A sulfite concentration of 10 mM suppresses significantly rel. $[H_2O_2]_i$ below baseline values. $^*P < 0.05$; $^{**}P < 0.01$; the Behrens-Fischer significance test and error propagation define the error bars shown.

Fluo-3 (22, 23), Fura-red (24), and Indo-1 (25,26). Besides Fura-2, Indo-1 has the advantage of using the ratiometric method for detecting changes of intracellular free Ca^{2+} concentrations.

In our hands, FMLP-stimulated Ca^{2+} signals in PMN reach a maximum after 3 s, followed immediately by a biphasic return to baseline levels composed of an initial fast component and a subsequent slower decrease. Taking into account the sample transportation time to the laser intersection point, this behavior is in accordance with the results of Hallet et al. (2,16). They found a mean lag time in PMN for a Ca^{2+} response to FMLP of 530 ms within a range from 75 to 1,500 ms.

Fluorescent probes are widely used for the measurement of ROI (10,27–29). To study kinetics of the respiratory burst, chemiluminescence (21) or the reduction of cytochrome C (17,30) was commonly used. Comparable experiments with fluorescent probes have rarely been performed (31). For our purposes, DHR-123 is the fluorescence dye of choice, due to its stability, specificity, and high quantum yield (10,29). Our data show a small increase of fluorescence intensity over 17 min, even in sham-stimulated PMN, probably as a result of an endogenous baseline generation of ROI in unstimulated cells.

Few experiments use fluorescence dye double labeling to investigate intracellular free calcium and respiratory burst. Bueb et al. (32) developed a double-dye spectrofluorometric technique with Fura-2 and DHR-123, whereas Lund-Johansen and Olweus (24) used Fura-red and DHR-123 in a flow cytometric assay.

As stimuli of positive controls, FMLP and PMA are well known for testing phagocytic cell function. The chemotactic peptide FMLP activates PMN and monocytes via the formylpeptide receptor that mediates signal transduction pathways through GTP-binding proteins, leading to activation of NADPH oxidase. PMA is a soluble phorbol ester and activates PMN directly via protein kinase C (PKC) without involvement of a membrane-bound receptor. The activation by PMA also results in stimulation of the respiratory burst.

Respiratory burst occurs after stimulation with FMLP in PMN after a short lag time, with a steeper slope and higher level as in simultaneously stimulated monocytes. Together with the data from the simultaneously recorded Indo-1 fluorescence, it is evident that an increase of intracellular free calcium precedes the onset of FMLP- stimulated respiratory burst in both types of phagocytes.

In our opinion, an important approach is the simultaneous registration of the time-dependent fraction of responding cells with a time resolution of 1 s (Fig. 5). After stimulation with FMLP, a rapid onset was observed, followed by a gradual decline of the percentage of reacting cells, when regarding the concentration of intracellular free calcium. In contrast, when observing respiratory burst, there is an exponential rise of ROI in responding PMN and monocytes.

Analyzing the influence of the airborne pollutant sulfite, the range of relevant concentrations must be considered. In areas with high emission of combustion products, sulfur (IV) species might achieve levels up to 1–2 ppm. Some of these pollutants are adsorbed to respirable particles, which are deposited in the tracheobronchial tract. Under specific aerodynamic conditions in microcompartments of the peripheral airways, inhaled particles might locally accumulate and generate toxic levels of S(IV). In this regard, the in vitro effects of sulfite up to 1 mM concentration are considered to be relevant regarding aspects related to public health. The ef-

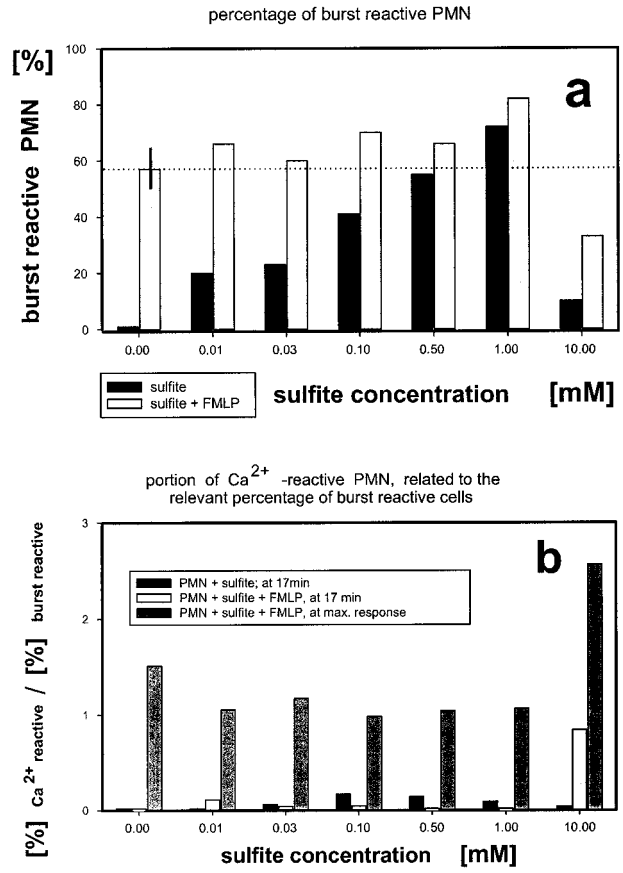

FIG. 9. Effects of sulfite on the fractions of burst-responding neutrophils. **a:** Data [%] relate to the sst-H_2O_2 fraction of responding cells (see Fig. 5b), corrected for DHR baseline control levels and the biological variance of blood donors by a factor D_{corr}, where $D_{corr} = F_{FMLP,mean}$ [%]/$F_{FMLP,i}$[%]. ($F_{FMLP,mean}$ is the mean FMLP-induced burst response of all PMN populations used—characterized by the dashed line—and $F_{FMLP,i}$ the corresponding value of every single preparation.) Sulfite alone in concentrations of 0.01–1.0 mM leads to an increase of the fraction of respiratory burst-reactive cells. A concentration of 10 mM diminishes this fraction. No dose dependence is observed when preincubation with sulfite occurs before stimulation with 10^{-7} M FMLP. **b:** Comparison of the fraction of Ca^{2+}-responding cells with the burst-responding cells. At the time interval between 900 and 1,023 s (related to sst-Ca^{2+} and sst-H_2O_2, respectively), the fractions of Ca^{2+} and burst-reactive neutrophils are independent of each other if stimulation occurs with sulfite alone or after preincubation with sulfite before FMLP stimulation. The value at a sulfite concentration of 10 mM, where 80% of the burst-reactive neutrophils show enhanced Ca^{2+} levels, is of minor importance: the portion of burst-reacting cells is just 30% (Fig. 9a). At the time point of maximal Ca^{2+} response, sulfite in concentrations of 0.01–1.0 mM leads to a ratio of Ca^{2+} to burst-reactive cells around 1. 10 mM sulfite causes a 2.6-fold increase of Ca^{2+} reactive neutrophils in comparison to the fraction of burst-reactive cells that were, however, reduced to 30%.

fect of higher concentrations is of theoretical interest, but might be relevant in genetic-associated deficiency of sulfite oxidase, an enzyme that is responsible for the detoxification of endogeneous S(IV).

Little is known about the direct effects of sulfite on the calcium homeostasis in PMN, although there is some experimental evidence of sulfite acting on PKC and Ca^{2+}/calmodulin-dependent pathways (5). As shown in our study, sulfite alone causes only a small spontaneous increase of intracellular free calcium. Effects of sulfite, alone and before stimulation with FMLP on the sst-Ca^{2+}, become significant with an increase of $[Ca^{2+}]_i$ only at high concentrations of 10 and 100 mM. These concentrations also cause a significant depression of the maximal Ca^{2+} peak related to FMLP. These alterations of calcium levels are possibly caused by an impairment of cellular energy metabolism, resulting in a significant decrease of intracellular ATP production (8,33).

The influence of sulfite on the generation of ROI in PMN has previously been investigated using the chemiluminegenic probes lucigenin and luminol (4,5,7) and a flow cytometric assay with dichlorofluorescein diacetate (DCFH-DA) (4). The optimal sulfite concentration for generating ROI is 1 mM when using lucigenin-dependent chemiluminescence or DCF fluorescence, comparable to our results with an optimal sulfite concentration between 0.1 and 0.5 mM. It is interesting to mention that sulfite has virtually no stimulating effect when measuring myeloperoxidase activity with luminol-dependent chemiluminescence. Control experiments have shown that this enzyme is completely inhibited by sulfite (7). In our hands, preincubation with sulfite in concentrations of 0.001–5.0 mM has an additive effect on ROI production when stimulated with FMLP. A sulfite concentration of 10 mM suppresses significantly the generation of reactive oxygen species below baseline levels in unstimulated PMN and, to an even greater extend, in FMLP-stimulated cells. As shown by Beck-Speier et al. (8), PMN are devoid of the sulfite-detoxifying enzyme sulfide oxidase, which is responsible in a reciprocal relationship for the sensitivity of the energy metabolism to sulfite. Tissues and cells endowed with low sulfite oxidase activity showed a substantial loss of ATP at high sulfite concentrations (4,8). Depletion of cellular ATP content, however, diminishes available NADPH equivalents necessary for NADPH oxidase-catalyzed reduction of oxygen to ROI (5). A dramatic NADPH depletion after FMLP stimulation of PMN was also experimentally shown by Liang and Petty (34).

Our findings that high sulfite concentrations (10 mM) substantially suppress the respiratory burst response of PMN below baseline level are in agreement with these observations. Our data, however, are in contrast to those reported by Labbe et al. (6), who described a substantial stimulation of the respiratory burst by 10 mM sulfite. Reasons for this discrepancy might be different conditions during cell incubations (pH, composition of medium) or the method of ROI determination. It shoud be mentioned that sulfite interferes with the reduction of cytochrome C, a well-known method for measuring superoxide anions. Chemiluminescence measurements used by Beck-Speier et al. (4,5) and fluorescence measurements presented in this article, however, are not directly affected by sulfite.

In our opinion, the analysis of the fractions of responding cells, in regard to simultaneous measurements of reactions on given stimuli, is a new aspect (Fig. 9a). Our data show that sulfite in concentrations up to 1.0 mM not only enhances the generation of ROI, but also increases the fraction of responding PMN from 0% up to 70% at maximum response. Probably

due to energy depletion, only 10% of PMN generate ROI when treated with 10 mM sulfite. Investigating the effects of sulfite preincubation, no correlation could be observed between the percentage of burst-reactive PMN stimulated with FMLP and sulfite concentration.

Comparing the fraction of Ca^{2+}-reactive PMN in relation to the relevant percentage of burst-reactive cells (Fig. 9b), our data do not show any relationship between Ca^{2+} and burst-reactive PMN at the steady-state levels after treatment with sulfite alone or after preincubation prior to FMLP stimulation. This means that sulfite does not markedly influence Ca^{2+} metabolism at concentrations up to 1 mM. However, there is a significant effect on oxidative defense mechanisms. The data presented in this study, indicating the absence of a Ca^{2+} transient by sulfite, suggest a direct action of sulfite on PKC. This pathway is comparable to the effect of PMA, which stimulates oxidative burst via PKC activation without generating Ca^{2+} transients.

Considering the time point of maximal Ca^{2+} response elicited through FMLP after preincubation with sulfite, it is remarkable that sulfite up to 1 mM synchronizes respiratory burst and that Ca^{2+}-responding cells, i.e., all burst-reactive cells, are simultaneously Ca^{2+} reactive. In contrast, after preincubation with 10 mM sulfite, which substantially depletes cellular ATP content (5,8), 2.6-fold more PMN exhibit a Ca^{2+} reaction than a respiratory burst. These aspects lead to the possible explanation that in cases of low available energy equivalents in PMN, upon stimulation with FMLP, a reduction of the maximal Ca^{2+} response is followed by a significantly elevated sst-Ca^{2+} (Fig. 7b), whereas the generation of ROI, as a more downstream part of signal transduction, is virtually abolished (Fig. 8c).

ACKNOWLEDGMENTS

We thank Mr. O. Lock for his excellent technical assistance in developing the thermostatted sample holder. The fruitful comments of M. Nuesse are gratefully acknowledged.

LITERATURE CITED

1. Sibille Y, Marchandise F-X. Pulmonary immune cells in health and disease: polymorphonuclear neutrophils. Eur Respir J 1993;6:1529–1543.
2. Hallet MB, Lloyds D. The molecular and ionic signalling of neutrophils. Heidelberg: Springer Verlag; 1997.
3. Ricevuti G, Pasotti D, Kowolik MJ, Mazzone A. Clinical manifestations of neutrophil leukocyte dysfunction. Int J Immunopathol Pharmacol 1993;6:199–230.
4. Beck-Speier I, Lenz A-G, Godleski JJ. Responses of human neutrophils to sulfite. J Toxicol Environ Health 1995;41:285–297.
5. Beck-Speier I, Liese JG, Belohradsky BH, Godleski JJ. Sulfite stimulates NADPH oxidase of human neutrophils to produce active oxygen radicals via protein kinase C and Ca^{2+}/calmodulin pathways. Free Radic Biol Med 1993;14:661–668.
6. Labbe P, Pelletier M, Omara FO, Girard D. Functional responses of human neutrophils to sodium sulfite (Na_2SO_3) in vitro. Hum Exp Toxicol 1998;17:600–605.
7. Mishra A, Dayal N, Beck-Speier I. Effect of sulphite on the oxidative metabolism of human neutrophils: studies with lucigenin- and luminol-dependent chemiluminescence. J Biolumin Chemilumin 1995;10:9–19.
8. Beck-Speier I, Hinze H, Holzer H. Effect of sulfite on the energy metabolism of mammalian tissues in correlation to sulfite oxidase. Biochim Biophys Acta 1985;841:81–89.
9. Grynkiewicz G, Poenie M, Tsien RY. A new generation of Ca^{2+} indicators with greatly improved fluorescence properties. J Biol Chem 1985;260:3440–3450.
10. Rothe G, Oser A, Valet G. Dihydrorhodamine 123: a new flow cytometric indicator for respiratory burst activity in neutrophil granulocytes. Naturwissenschaften 1988;75:354–355.
11. Grundler W, Dirscherl P, Beisker W, Marx K, Stampfl A, Maier K, Zimmermann I, Nüsse M. Early functional apoptotic responses of thymocytes analysed by time-resolved flow cytometry Cytometry (in press).
12. Beisker W. A new combined integral-light and slit scan data analysis system (DAS) for flow cytometry. Comput Methods Programs Biomed 1994;42:15–26.
13. Campbell RC. Statistics for biologists. London: Cambridge Unviersity Press; 1967.
14. June CH, Rabinovitch PS. Intracellular ionized calcium. In: Darzynkiewicz Z, Robinson JP, Crissman HA, editors. Methods in cell biology, Vol. 41. San Diego: Academic Press; 1994. p 149–174.
15. Gomes PAP, Bassani RA, Bassani JWM. Measuring Ca^{2+} with fluorescent indicators: theoretical approach to the ratio method. Cell Calcium 1998;24:17–26.
16. Hallett MB, Davies EV, Campbell AK. Oxidase activation in individual neutrophils is dependent on the onset and magnitude of the Ca^{2+} signal. Cell Calcium 1990;11:655–663.
17. Korchak HM, Vosshall LB, Haines KA, Wilkenfeld C, Lundquist KF, Weissmann G. Activation of the human neutrophil by calcium-mobilizing ligands. J Biol Chem 1988;263:11098–11105.
18. Nielsen OH, Bouchelouche PN, Berild D, Ahnfelt-Ronne I. Effect of 5-aminosalicylic acid and analogous substances on superoxide generation and intracellular free calcium in human neutrophilic granulocytes. Scand J Gastroenterol 1993;28:527–532.
19. Petersen M, Williams JD, Hallett MB. Cross-linking of CD11b or CD18 signal release of localized Ca^{2+} from intracellular stores in neutrophils. Immunology 1993;80:157–159.
20. Rosales C, Brown EJ. Calcium channel blockers nifedipine and diltiazem inhibit Ca^{2+} release from intracellular stores in neutrophils. J Biol Chem 1992;267:1443–1448.
21. Tuomala M, Hirvonen M-R, Savolainen KM. Changes in free intracellular calcium and production of reactive oxygen metabolites in human leukocytes by soluble and particulate stimuli. Toxicology 1993;80:71–82.
22. Merritt JE, McCarthy SA, Davies MPA, Moores KE. Use of fluo-3 to measure cytosolic Ca^{2+} in platelets and neutrophils. Biochem J 1990;269:513–519.
23. Elsner J, Kaever V, Emmendörffer A, Breidenbach Th, Lohmann-Matthes ML, Roesler J. Heterogeneity in the mobilization of cytoplasmic calcium by human polymorphonuclear leukocytes in response to FMLP, C5a and IL-8/NAP-1. J Leukoc Biol 1992;51:77–83.
24. Lund-Johansen F, Olweus J. Signal transduction in monocytes and granulocytes measured by multiparameter flow cytometry. Cytometry 1992;13:693–702.
25. Lopez M, Olive D, Mannoni P. Analysis of cytosolic ionized calcium variation in polymorphonuclear leukocytes using flow cytometry and Indo-1 AM. Cytometry 1989;10:165–173.
26. Norgauer J, Krutmann J, Dobos GJ, Traynor-Kaplan AE, Oades ZG, Schraufstätter IU. Actin polymerization, calcium-transients, and phospholipid metabolism in human neutrophils after stimulation with interleukin-8 and N-formyl peptide. J Invest Dermatol 1994;102:310–314.
27. Emmendörfer A, Hecht M, Lohmann-Matthes M-L, Roesler J. A fast and easy method to determine the production of reactive oxygen intermediates by human and murine phagocytes using dihydrorhodamine 123. J Immunol Methods 1990;131:269–275.
28. Himmelfarb J, Hakim RM, Holbrook DG, Leeber DA, Ault KA. Detection of granulocyte reactive oxygen species formation in whole blood using flow cytometry. Cytometry 1992;13:83–89.
29. Vowells SJ, Sekhsaria S, Malech HL, Shalit M, Fleisher TA. Flow cytometric analysis of the granulocyte respiratory burst: a comparison study of fluorescent probes. J Immunol Methods 1995;178:89–97.
30. Lundqvist H, Gustafsson M, Johansson A, Särndahl E, Dahlgren C. Neutrophil control of formylmethionyl-leucyl-phenylalanine induced mobilization of secretory vesicles and NADPH-oxidase activation: effect of an association of the ligand-receptor complex to the cytoskeleton. Biochim Biophys Acta 1994;1224:43–50.
31. van Pelt LJ, van Zwieten R, Weening RS, Roos D, Verhoeven AJ, Bolscher BGJM. Limitations on the use of dihydrorhodamine 123 for flow cytometric analysis of the neutrophil respiratory burst. J Immunol Methods 1996;191:187–196.
32. Bueb J-L, Gallois A, Schneider J-C, Parini J-P, Tschirhart E. A double-labelling fluorescent assay for concomitant measurements of $[Ca^{2+}]_i$ and O_2 production in human macrophages. Biochim Biophys Acta 1995;1244:79–84.
33. Maier K, Hinze H, Leuschel L. Mechanism of sulfite action on the energy metabolism of *Saccharomyces cerevisiae*. Biochim Biophys Acta 1986;848:120–130.
34. Liang B, Petty HR. Imaging neutrophil activation: analysis of the translocation and utilization of NAD(P)H-associated autofluorescence during antibody-dependent target oxidation. J Cell Physiol 1992;152:145–156.